

AUTOMATIC DRIVING COMFORT ANALYSIS AND INTELLIGENT IDENTIFICATION OF UNCOMFORTABLE MANOEUVRES BASED ON VEHICLE-FOLLOWING SCENARIO

JIACHENG FENG

China Intelligent and Connected Vehicles, Research Institute Co., Ltd., Beijing, China

e-mail: fengjiacheng@china-icv.cn

Driving comfort and performance is of vital importance to evaluate the control quality of an automatic driving system. The control quality and calibration of the automatic driving system not only affects comfort but also psychological load and tension. Therefore, this paper proposed an analysis method of driving comfort combined with subjective and objective factors, including multidimensional analysis based on the velocity domain, acceleration energy and power analysis, perceived risk and deviation analysis. Moreover, the feature of typical uncomfortable manoeuvres is analysed and generates an intelligent identification algorithm. It has been found that the uncomfortable identification performance is excellent (the accuracy reached 99%).

Keywords: automatic driving, driving comfort, evaluation algorithm, wavelet filtering, neural network

1. Introduction

With the maturity of automatic driving technology and mass production, the driving comfort has become the key to evaluate the control quality of the system. It affects the physiological comfort and psychological load of drivers and passengers during automatic driving. Therefore, more and more researches are carried out on comfort and calibration of automatic driving systems, and test works have also become necessary. Burkhard *et al.* (2018) considered that passenger movements caused by accelerations of the body were essential pre-requisite for the ride comfort of autonomous vehicles. Wang *et al.* (2019) developed a comfort level model of autonomous vehicles through data acquisition and structure modeling and used an automatic scoring tool to guide technological development, optimize algorithms and improve strategies. Yusof *et al.* (2016) carried out research on the relationship between different driving styles (assertive and defensive) and comfort. They improved the comfort performance through the study of driving behavior of an autonomous vehicle.

Most of the evaluation methods are based on qualitative analysis, and the quantitative analysis does not extract and decompose the features of uncomfortable conditions to study its typical characteristics. In addition, there are few studies on multi-domain quantitative analysis of vehicle-following scenarios and there is a lack of the research on typical uncomfortable manoeuvres perceived by human.

Therefore, this paper proposes quantitative analyses based on the time and velocity domain combined with subjective empirical data from automobile enterprises. In addition, the feature formula of uncomfortable manoeuvres in the test is established, and the intelligent identification network of these manoeuvres is trained by a neural network algorithm. In general, the traditional driving comfort evaluation depends on the subjective feelings of the evaluators, and there are certain individual differences and unreliability. The methodology and algorithm proposed

in this paper avoid human factors by forming a consistent evaluation standard and show the system calibration characteristics through quantitative distribution. Especially for uncomfortable working conditions, the amplitude change and variable correlation can be analyzed by data figures, which is significant for the calibration tendency and control characteristics of the system under the test. At the same time, the trained identification network can effectively extract the uncomfortable manoeuvres from the test data automatically.

2. Analysis and evaluation method

The uncomfortable working condition is mainly caused by acceleration value and variation characteristics during driving, especially in the direction of driving for automatic driving vehicles. Therefore, the analysis of acceleration and the characteristics of uncomfortable manoeuvres are the key points. To generate a scientific and quantitative method, the analysis architecture and flow based on the time domain and velocity domain are established.

Test data reconstruction and statistical calculation were used for acceleration analysis. The uncomfortable manoeuvres output analysis is evaluated by acceleration energy and power. The risk perception analysis is calculated by a weighting function, the empirical thresholds are introduced for the deviation dynamic analysis. As shown in Fig. 1a, the test data is filtered and transformed in the velocity domain, then carry out the analysis of acceleration multidimensional distribution, energy and power, perceived risk and comfort.

Moreover, based on the analysis of uncomfortable manoeuvres data, an artificial intelligence algorithm is introduced to generate the feature network for automatic identification of such manoeuvres. A two-layer neural net is constructed for training based on the feature data of typical uncomfortable manoeuvres. The architecture and flow are shown in Fig. 1b which includes test data preprocessing, feature extraction, network design and training, the result test and validation.

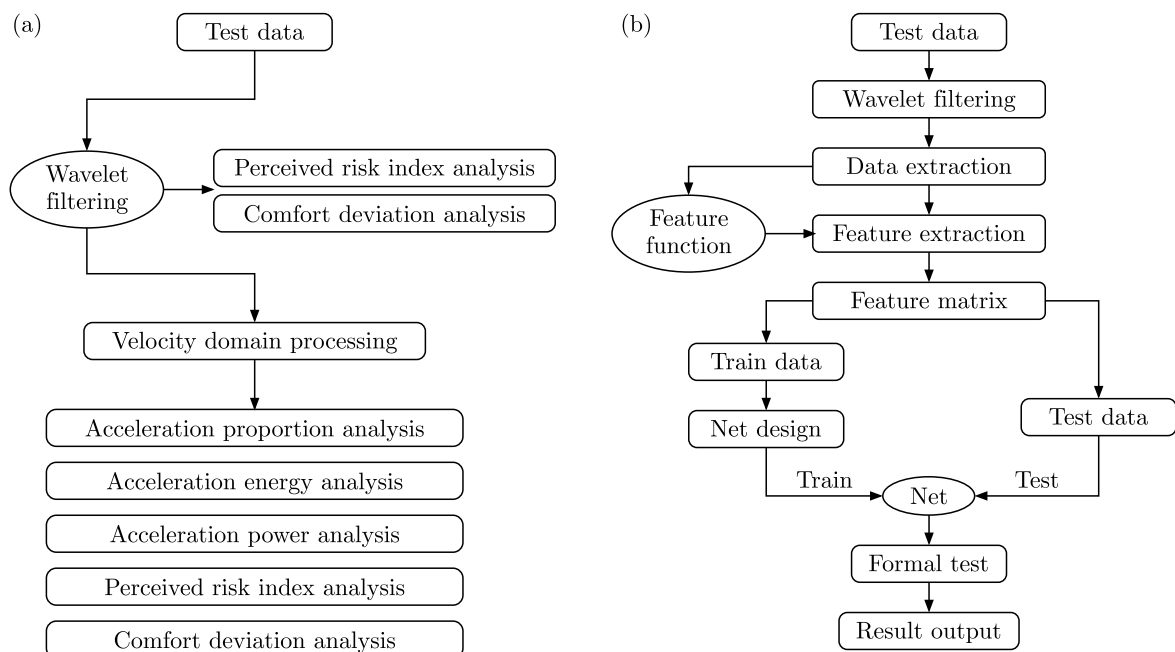


Fig. 1. Analysis and evaluation logical architecture

3. Test and filtering processing

3.1. Test scenario

In order to simulate typical urban traffic conditions, a periodic acceleration and deceleration vehicle-following scenario is used to perform the test. Through the manoeuvre design of the leading vehicle to guide the host vehicle (automatic driving vehicle under test), the control strategy and manoeuvre response is indirectly analyze. The test scenario is shown in Fig. 2, the parameter setting of the leading vehicle is shown in Table 1 (Didier and Landau, 2005; Tang *et al.*, 2017).

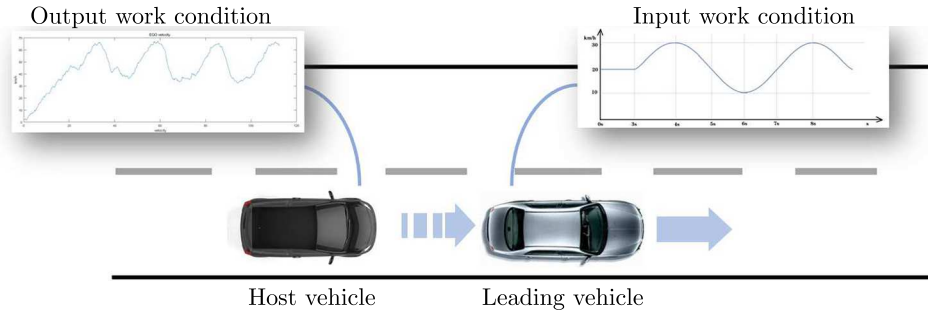


Fig. 2. Longitudinal velocity of the interactive vehicle

Table 1. Interactive vehicle parameter setting

Velocity range	40-60 km/h
Cycle period	8 s
Experiment distance	1400 m
Road type	long straight road
Route plan	straight line
Initial velocity	0 km

3.2. Test data preprocessing

3.2.1. Filtering algorithm

Due to the interference of test facility noise and vibration of the fixed mechanism, the original signal needs denoising and smoothing for subsequent analysis. The discomfort and motion sickness of the automatic driving vehicle in the driving direction is mainly affected by low-frequency acceleration. For this reason, it is necessary to reject the interference of high-frequency noise. In signal processing, the wavelet transform has the advantage of noise reduction and protects the spike and transient signals (Hazarika *et al.*, 1997). Therefore, this method is used to process the original acceleration data through the test.

The discrete wavelet function is shown in Eq. (3.1), where $\Psi(t)$ denotes the integral wavelet, t denotes time, a denotes the scale and b denotes the offset, j denotes the scaling of the wavelet function in the frequency domain and k denotes translation of the function in the time domain

$$\Psi_{j,k}(t) = a_0^{-j/2} \Psi(a_0^{-j} t - kb_0) \quad j, k \in Z \quad (3.1)$$

The discrete wavelet transform coefficients W is

$$W_{j,k}(t) = \int_{-x}^{\infty} f(t) \Psi_{j,k}(t)^* dt \quad (3.2)$$

The coefficient reconstruction formula of the discrete wavelet transform is shown in Eq. (3.3), C denotes a constant independent of the signal (Rioul and Vetterli, 1991)

$$f(t) = C \sum_{-\infty}^{\infty} \sum_{-\infty}^{\infty} W_{j,k} \Psi_{j,k}(t) \quad (3.3)$$

3.2.2. Calculation

In this paper, the daubechies (dbN) wavelet is selected in calculation, N (db number) is the number of vanishing moments. Basically, the higher the number of vanishing moments, the smoother the wavelet. The level is the number of decomposition layers. The more layers, the more high-frequency components filtered, but the greater the difference between the low-frequency results and the original signal (Guan *et al.*, 2015). In the paper, we set $N = 4$ and decomposition level to 4. The calculation result shown in Fig. 3a is a wavelet tree. Figure 3b shows the test raw data collected by test facility, Fig. 3c the processed data. It can be seen from the curve of processed data that the high-frequency clutter is eliminated, and the data curve is smoother, which is a conducive feature in the analysis (Cai *et al.*, 2003).

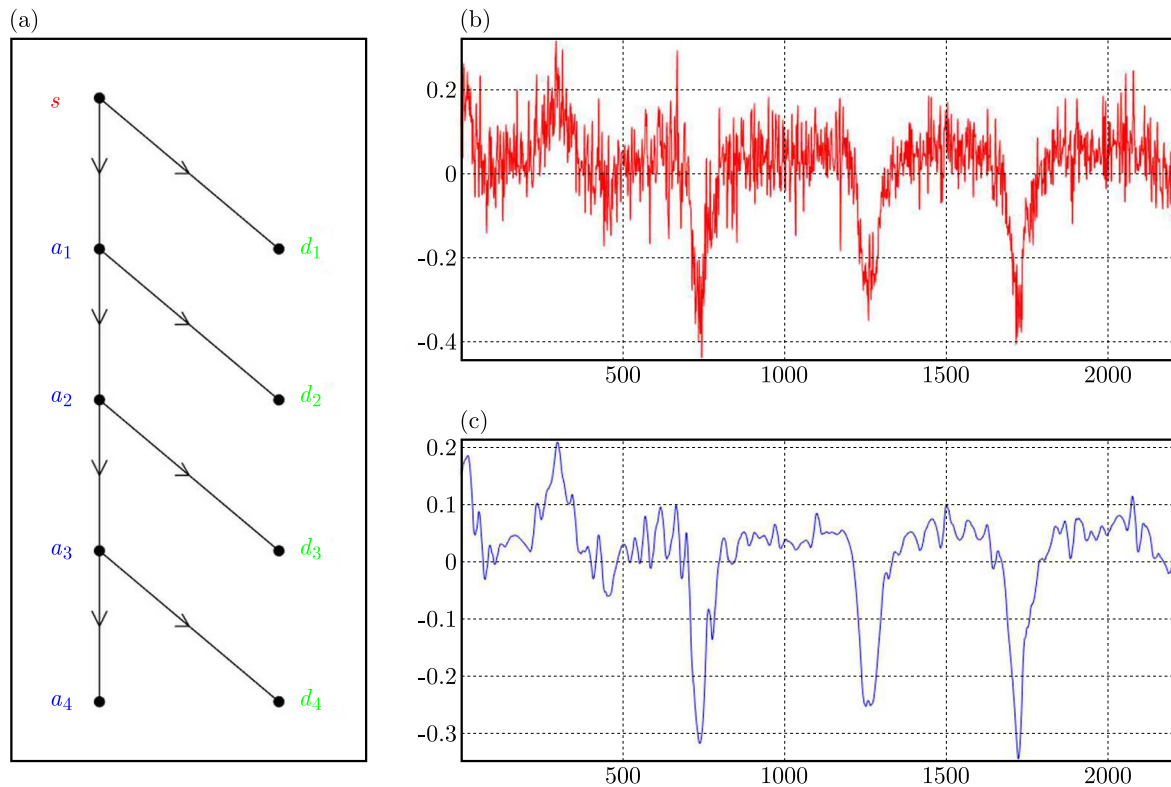


Fig. 3. Decomposition at 4 levels: (a) wavelet tree, (b) signal, (c) approximation at level 4 (reconstructed)

4. Comfort analysis based on the velocity and time domain

4.1. Acceleration proportion analysis

The analysis based on the velocity domain is significant for a vehicle-following scenario because the control response of the host vehicle is different at different velocity. Under the vehicle-following scenario, the acceleration distribution and proportion in the velocity domain

can comprehensively present the automatic driving performance of the host vehicle. The calculation is shown in Eq. (4.1), n_c denotes the number of sampling points under the corresponding condition, n_{total} denotes the total number of sampling points

$$f(v, a) = \frac{n_c |condition}{n_{total}} \quad condition : \begin{cases} v(i) \in (i, i + e_v] & \text{for } i \in [1, n_v] \\ a(j) \in (j, j + e_a] & \text{for } j \in [1, n_a] \end{cases} \quad (4.1)$$

The calculation result is shown in Fig. 4, x -axis and y -axis represent velocity and acceleration respectively, z -axis represents the proportion under the current acceleration and velocity values in this scenario. The figure can be used to evaluate the comfort performance of the system at different following velocities. The characteristics of good control performance are a small proportion of high acceleration and distribution characteristics of a low acceleration area at high velocity. The figure shows that the higher acceleration is relatively concentrated between 30-60 km/h and accounts for a large proportion in the low value area (0-1.5 m/s²). The maximum measured acceleration (2.5-3.5 m/s²) occurs in the range of 40-60 km/h, in which there are the aggressive braking manoeuvres when the leading vehicle suddenly decelerates according to the test process.

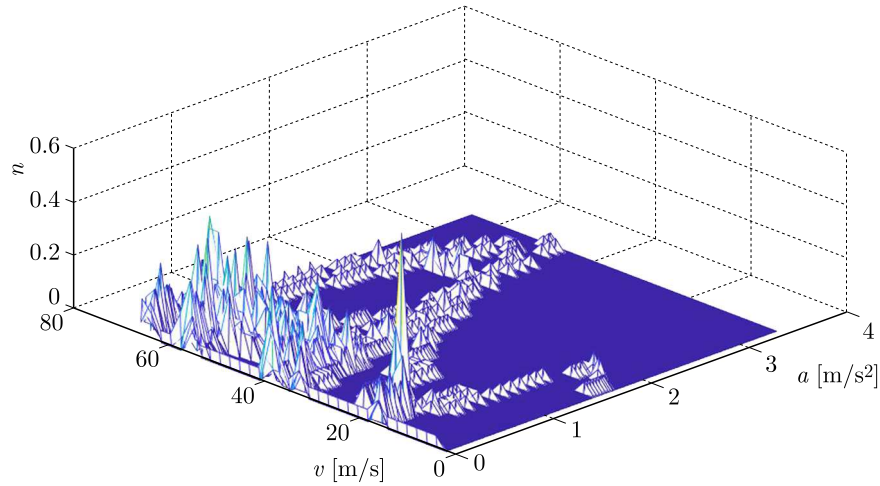


Fig. 4. Acceleration-velocity-proportion map

4.2. Acceleration energy map and power analysis

Acceleration energy can quantify the cumulative output of acceleration in different velocity ranges. In addition, it reflects the degree of discomfort input by vehicle to drivers and passengers, the calculation result is shown in Eq. (4.2). In each range of the velocity, $a_i(v)$ denotes the acceleration value per sample, m denotes the sample number, $E(i)$ denotes the energy. Figure 5a shows that high energy areas are distributed around 10, 30 and 60 km/h

$$E(i) = \sum_1^m a_i^2(v) \quad a_i \in (0, \max(a_i)) \quad (4.2)$$

The acceleration power represents the discomfort intensity in each velocity range. The calculation results of acceleration power are presented as Eq. (4.3), where $P(i)$ is the power of the current unit velocity. Figure 5b shows that the high-power work condition is concentrated below 10 km/h. Based on human's psychological hint between velocity and risk, high-energy acceleration in the high-velocity scenario will bring more tension and be uncomfortable to drivers and passengers than in the low-velocity scenario. Therefore, the energy and power output perfor-

mance in the high-velocity range is well-controlled, and the uncomfortable manoeuvres tend to the low-velocity range (Kusmirek *et al.*, 2016; Zhao *et al.*, 2013; Rihaczek, 1968)

$$P(i) = \frac{1}{m} \sum_1^m a_i^2(v) \quad a_i \in (0, \max(a_i)) \quad (4.3)$$

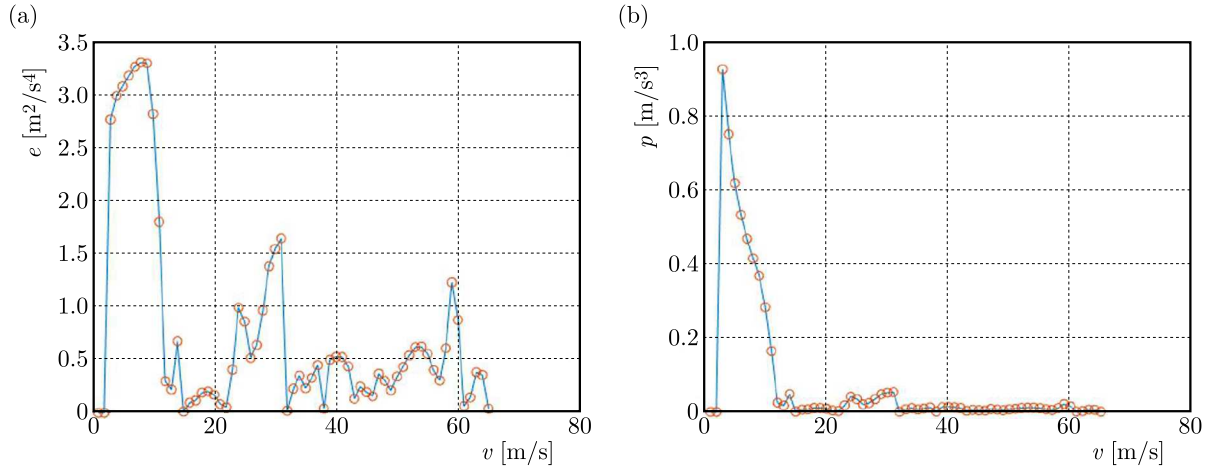


Fig. 5. Acceleration energy (a) and power (b)

4.3. Perceived risk index and comfort deviation analysis

Drivers and passengers have a positive psychological mapping relationship between velocity and risk. The faster the velocity, the greater perceived risk and tension. In addition, large acceleration fluctuation at high velocity will increase the driver's psychological load. Therefore, a good dynamic control strategy is to minimize the aggressive control under the high-velocity condition. Then, the calculation method of the perceived risk index $P_n(t)$ is proposed, as shown in Eq. (4.4)₁, which is calculated by multiplying the acceleration $a(t)$ and velocity coefficient $v_n(t)$. $v_n(t)$ is the normalization of velocity (in the velocity range of 0-120 km/h), the calculation is shown in Eq. (4.4)₂. The result in the time domain is shown in Fig. 6a. Obviously, the index value is relatively high in the three scenarios with high-velocity aggressive braking, at 36 s, 62 s and 86 s, respectively

$$p_n(t) = a(t)v_n(t) \quad v_n(t) = \frac{v(t)}{v_{max}} \quad (4.4)$$

Based on subjective perception empirical data of velocity and acceleration (from a Japanese automaker), the perceived risk deviation analysis is proposed to extract the obviously uncomfortable manoeuvres. The threshold function of perceived comfort is constructed as shown in Eq. (4.5)₁, where a_w is the empirical thresholds, and where a_1 , a_2 , a_3 are the maximum thresholds of subjective comfort in different velocity ranges. The comfort deviation value $P_d(t)$ is the difference between $P_n(t)$ and $P_w(t)$, the calculation result is shown in Eq. (4.5)₂. If $P_d(t) \geq 0$, it means that the vehicle manoeuvre is in the acceptable range. If $P_d(t) < 0$, it means that the vehicle performs obviously uncomfortable manoeuvres. The smaller the value, the more uncomfortably the driver feels. The calculation result in the time domain is shown in Fig. 6b, there are three obviously uncomfortable manoeuvres corresponding to Fig. 3

$$p_w(v) = a_w v_n(t) \quad a_w = \begin{cases} a_1 & \text{for } 0 < v_t \leq 40 \\ a_2 & \text{for } 40 < v_t \leq 80 \\ a_3 & \text{for } 80 < v_t \leq 120 \end{cases} \quad (4.5)$$

$$p_d(t) = p_n(t) - p_w(t)$$

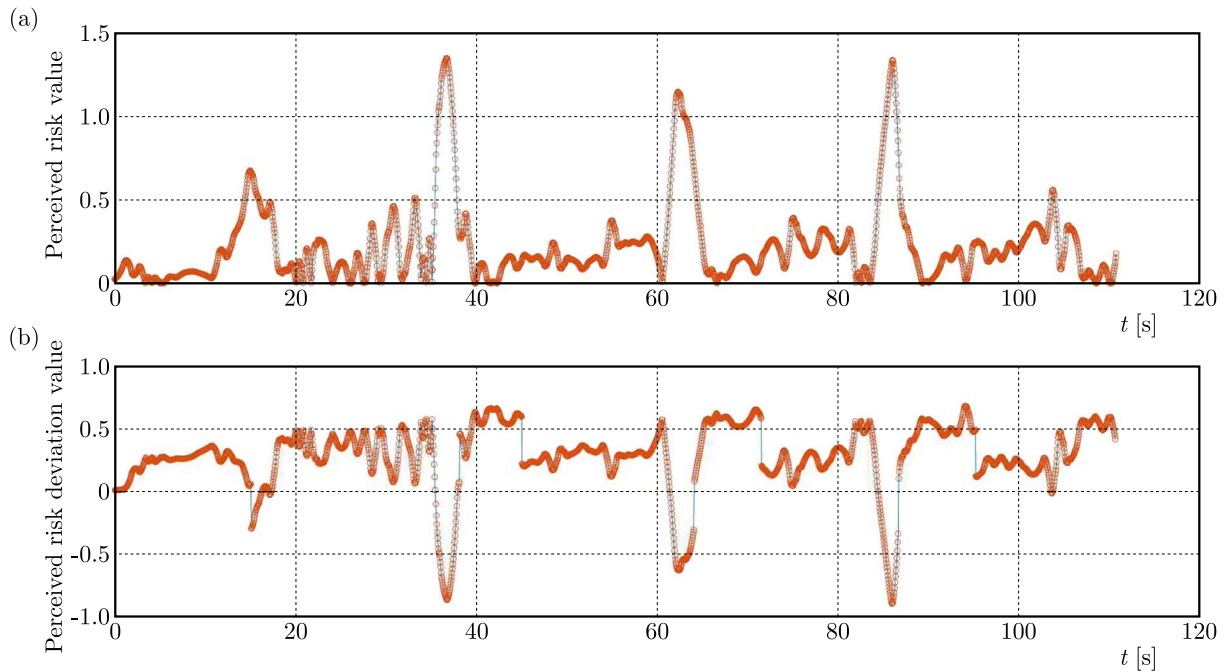


Fig. 6. Perceived risk and comfort deviations (time domain): (a) perceived risk index, (b) perceived risk deviation

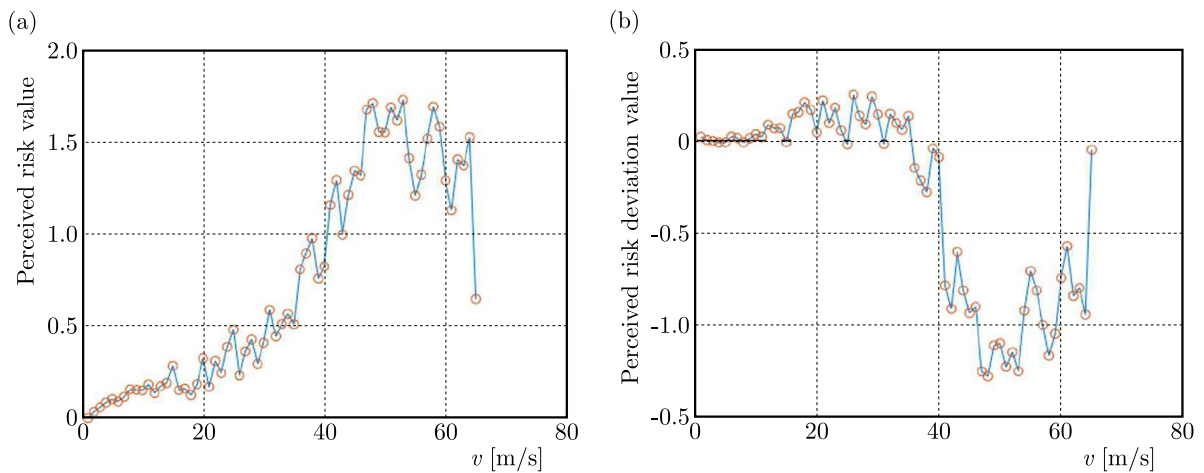


Fig. 7. Perceived risk and comfort deviations (velocity domain): (a) perceived risk index, (b) comfort deviation analysis

Perceived risk and comfort deviation analysis based on the velocity domain is calculated and plotted by extracting the maximum acceleration value of each velocity range, as shown in Fig. 7a and 7b. It can be seen from the figure that there are obviously uncomfortable manoeuvres in the velocity range of 40-60 km/h, which verifies consistency of the design scenario (aggressive acceleration and deceleration velocity range). The intensity of uncomfortable working conditions can be reduced by adjusting the vehicle-following sensitivity without affecting the traffic efficiency.

5. Intelligent identification of uncomfortable manoeuvres

5.1. Data feature extraction

In vehicle-following tests, the acceleration and deceleration manoeuvres causing physical discomfort and tension are extracted based on subjective feelings. The overlapping of these scenarios in terms of acceleration curves (gray curves) is shown in Fig. 8. We can find that the process basically belongs to V-shaped acceleration curve which including deceleration increase and decrease phases. Through analysis of the key influencing factors, the features of the simplified manoeuvre model are defined, as shown in Fig. 8.

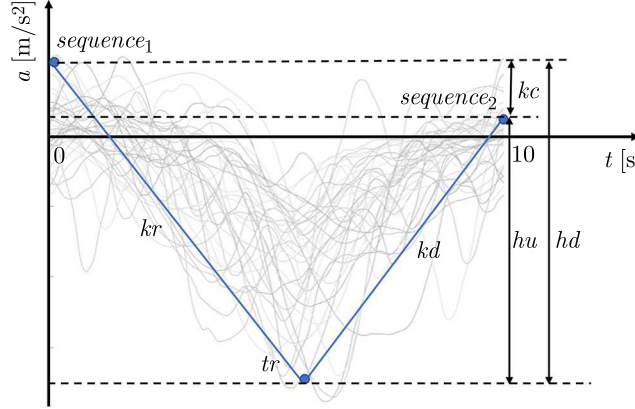


Fig. 8. Uncomfortable manoeuvre model feature design

Equation (5.1) enable calculation of these feature values, where tr is the minimum value in the data segment, kr and kd are deceleration increasing and decreasing slopes respectively, kc is the changing range between kr and kd , hu is the growth range between the end point and minimum value, hd is the reduction range between the starting point and minimum value. These feature values constitute the unit feature matrix \mathbf{S}_i of the extracted data segment

$$\begin{aligned}
 tr_i &= \min(sequence_i) & kr_i &= \frac{(tr_i - sequence_i(1))}{t_d - t_{amin}} \\
 kd_i &= \frac{(sequence_i(200) - tr_i)}{t_d - t_{amin}} & kc_i &= kd_i - kr_i \\
 hu_i &= tr_i - sequence_i(1) & hd_i &= sequence_i(200) - tr_i
 \end{aligned} \tag{5.1}$$

and

$$\mathbf{S}_i = [tr_i, kr_i, kd_i, kc_i, hu_i, hd_i]^T \tag{5.2}$$

In the experiment, uniform size data sets were used as units for data training and calculation of an artificial intelligence algorithm. $sequence_i$ is the data set generated by sequential data extraction in the chronological order. Each data set consists of i -th to $(i+m)$ -th samples in the whole scenario data, as shown in Fig. 9. The unit feature matrixes constitute the total feature matrix \mathbf{D}_h , Eq. (5.3)₁. In Eq. (5.3)₂, \mathbf{Y}_h is the judgment matrix corresponding to the matrix \mathbf{D}_h by the column

$$\mathbf{D}_h = [S_1, S_2, \dots, S_{n1}] \quad \mathbf{Y}_h = [y_1, y_2, \dots, y_{n1}] \tag{5.3}$$

$[0, 1]^T$ and $[1, 0]^T$ represent these data fragments for uncomfortable and comfortable manoeuvres respectively, shown as

$$\mathbf{Y}_i = \begin{cases} [1, 0]^T & \text{uncomfortable} \\ [0, 0]^T & \text{acceptable} \end{cases} \tag{5.4}$$

In subsequent calculations, $\mathbf{Y}_i(1, 1)$ denotes the judgment result, \mathbf{D}_t is the test data of the formal experiment, as shown in the matrix

$$\mathbf{D}_t = [S_1, S_2, \dots, S_{n2}] \quad (5.5)$$

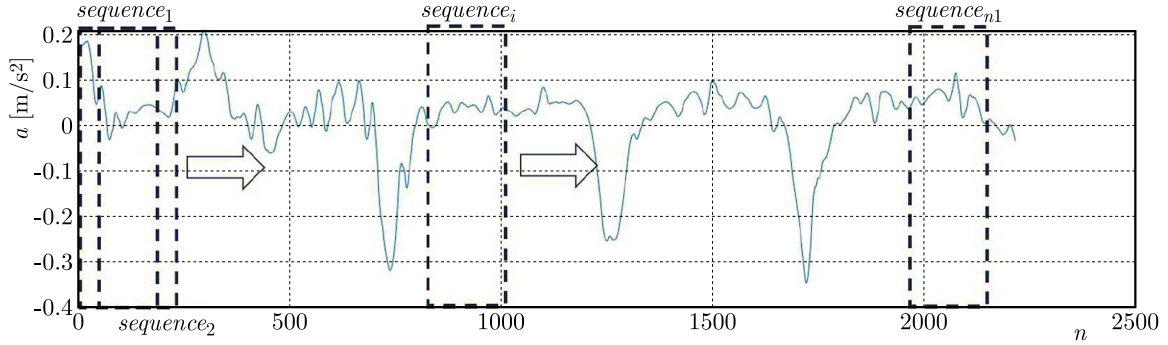


Fig. 9. Sequence data extraction

5.2. Algorithm design and training

Due to the fact that the quantitative equation for feature values cannot be established scientifically to identify such uncomfortable manoeuvres, the extracted features data is used for an artificial intelligence training algorithm to generate a feature network for automatic data analysis and recognition. In this paper, the identification network is generated by a machine learning algorithm of pattern recognition. Pattern recognition networks are feedforward networks that can be trained to classify inputs according to known target classes. These are two-layer feed-forward frameworks with sigmoid hidden and softmax output neurons, as shown in Fig. 10. The network is trained with scaled conjugate gradient backpropagation. The network attributes and parameter settings are shown in Table 2. The total number of training samples is 68 groups, 38 of which are uncomfortable manoeuvres and 30 groups are acceptable manoeuvres (Archer and Wang, 2010; Zhao, 2006; Liu *et al.*, 2008).

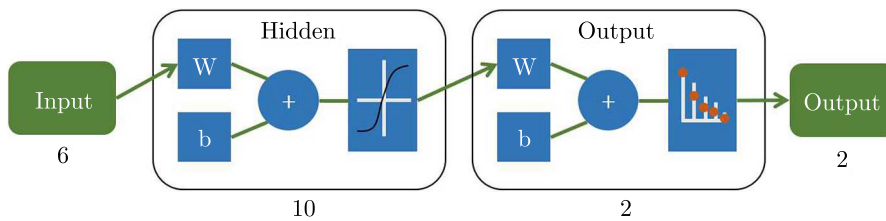


Fig. 10. Pattern recognition neural network

The summation function is Eq. (5.6), where ω and b denote the weight and bias of the neuron, respectively. The inputs matrix $\mathbf{S} = \{S_i\}$ is a set of values for which we need to predict the output value

$$z = \sum_{j=1}^6 \omega_j S_i(j) + b \quad (5.6)$$

The hidden layer adopts the sigmoid function as

$$a(z) = \frac{1}{1 + e^{-z}} \quad (5.7)$$

Table 2. Algorithm and parameter setting

Parameter	Setting
Trained function	scaled conjugate gradient
Cost function	cross-entropy function
Hidden layer size	10
Maximum training times	1000
Training set ratio	75%
Validation set ratio	15%
Test set ratio	15%

The hidden layer adopts the softmax function. The softmax value calculation of the element in the group is shown in Eq. (5.8), where i is the number of elements, v_i is the output value of the i -th node and c is the number of output samples

$$\text{Softmax}(v_i) = \frac{e^{v_i}}{\sum_{c=1}^c e^{v_j}} \quad (5.8)$$

The cost function adopts cross-entropy function shown in Eq. (5.9), where y denotes the corresponding actual value in the original data and m denotes the number of sample groups, g_i denotes the output value calculated through the node, h_θ is the hypothesis function to estimate the result

$$C = -\frac{1}{m} \left(\sum_{i=1}^m y_{(i)} \log h_\theta(g_i) + (1 - y_{(i)}) \log[1 - h_\theta(g_i)] \right) \quad (5.9)$$

In this paper, we use MATLAB as the algorithm training software. Through programming and multiple iterative calculations, the result shows that the number of iterations is 45 and the best validation performance is 0.03 at epoch 39. Figures 11 and 12 are the training result and accuracy of the generated net. The confusion matrix is Fig. 11, it denotes that accuracy of prediction results of the trained network is very high (error rate less than 2%). In Fig. 12, the ROC curve is very close to the upper left corner and almost at right angles, which denotes that the classifier network works well.

The generated network is expressed as I_0 , and the calculation is defined by Eq. (5.10)₁. For convenience of the expression, the output only extracts the first row of the result matrix (the identification result is 1 or 0), the calculation formula is expressed by Eq. (5.10)₂

$$I_0 = \text{net}(D_t) \quad I = I_0(1, j) \quad (5.10)$$

5.3. Error filtering algorithm design and calculation

In order to eliminate the unreasonable results caused by small amplitude uncomfortable manoeuvres, the filter function is designed for output data optimization. The function is shown in Eq. (5.11), the unit sampling data ranges $e = 20$ (i.e. 10 s). The average value of the data is considered valid when it is greater than 0.9, otherwise it is 0. In the formula, $i \in [1, n_2 - e]$, and the final automatic identification result is shown in Fig. 13. It can be seen from the figure that the three V-shaped acceleration waves with large amplitude changes are determined as uncomfortable manoeuvres for which the calculated result in the matrix is $W(i) = 1$. In addition, these identified ranges correspond to driver's subjective feeling of uncomfot and tension

$$W(i) = \begin{cases} I(i) & \text{for } \frac{1}{e} \sum_{k=i}^{i+e} I(k) > 0.9 \\ 0 & \text{for } \frac{1}{e} \sum_{k=i}^{i+e} I(k) \leq 0.9 \end{cases} \quad (5.11)$$

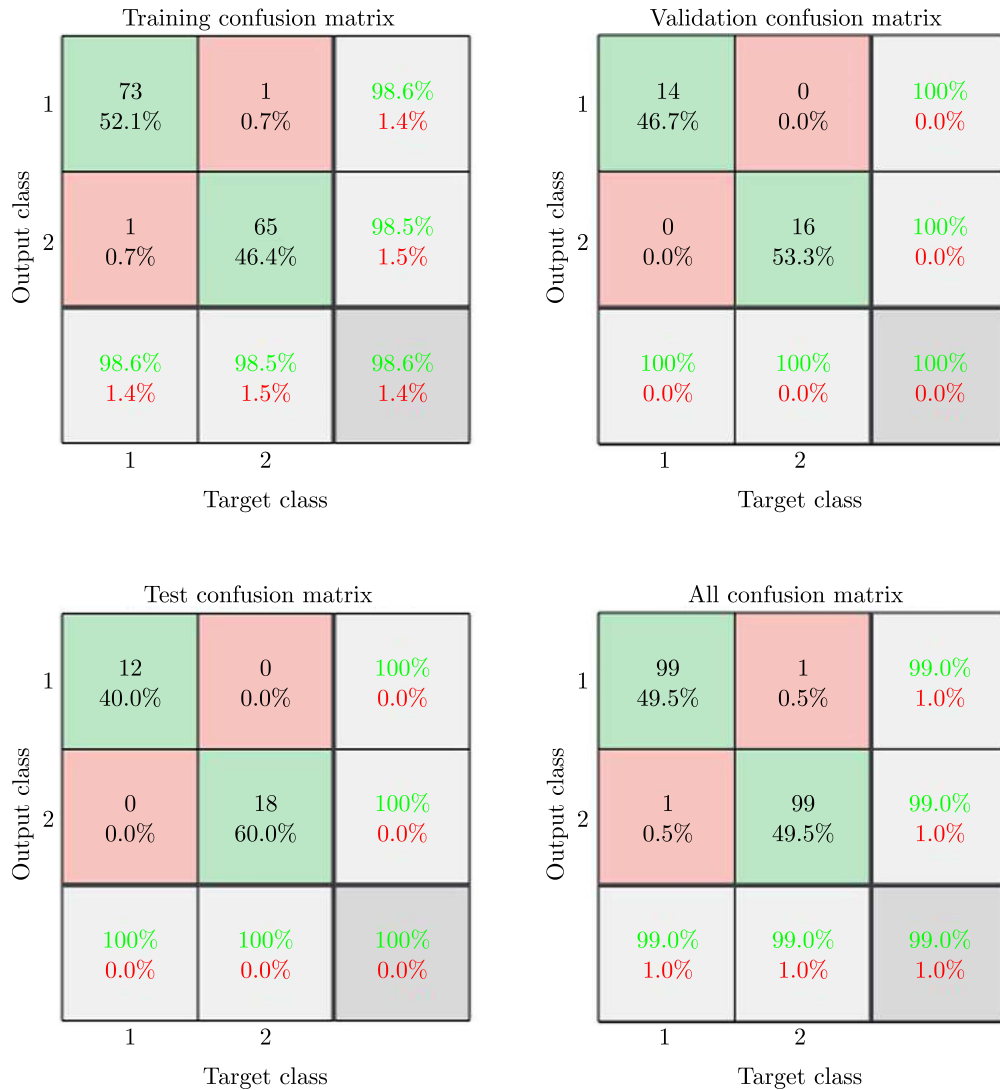


Fig. 11. Confusion matrix

6. Conclusions

This paper is a research on intelligent driving comfort and intelligent identification of uncomfortable manoeuvres. An innovative analysis method is proposed to show system calibration under typical city vehicle-following scenarios. In addition, a neural network is trained for intelligent identification of uncomfortable manoeuvres. The study in the paper has the following innovations and conclusions:

- Through data reconstruction, the control performance of dynamic acceleration is presented through a 3-dimensional distribution map. The result shows that the discomfort condition mainly occurs in the aggressive braking scenario of the leading vehicle. A suggestion for the improvement is that the control strategy of the host vehicle can more predictably identify the dynamics of the leading vehicle based on the velocity variation rate.
- Acceleration energy and power analysis present uncomfortable accumulated energy and intensity. The result shows ideal distribution characteristics reflecting the safety tendency and reasonable braking intensity distribution of the control strategy.
- Through combination of subjective feelings and an objective method, the driver's perceived risk and its deviation are dynamically analyzed. The braking conditions bring great

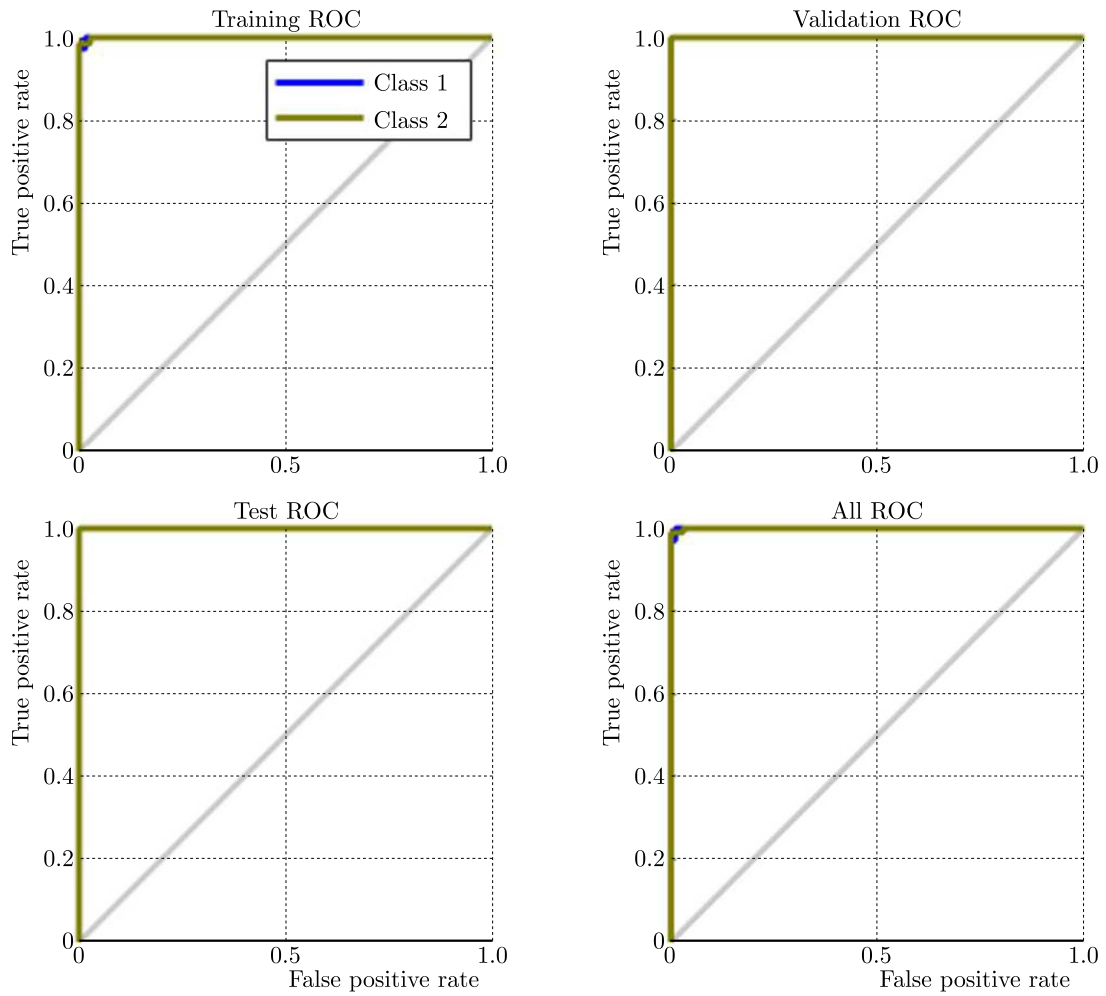


Fig. 12. ROC

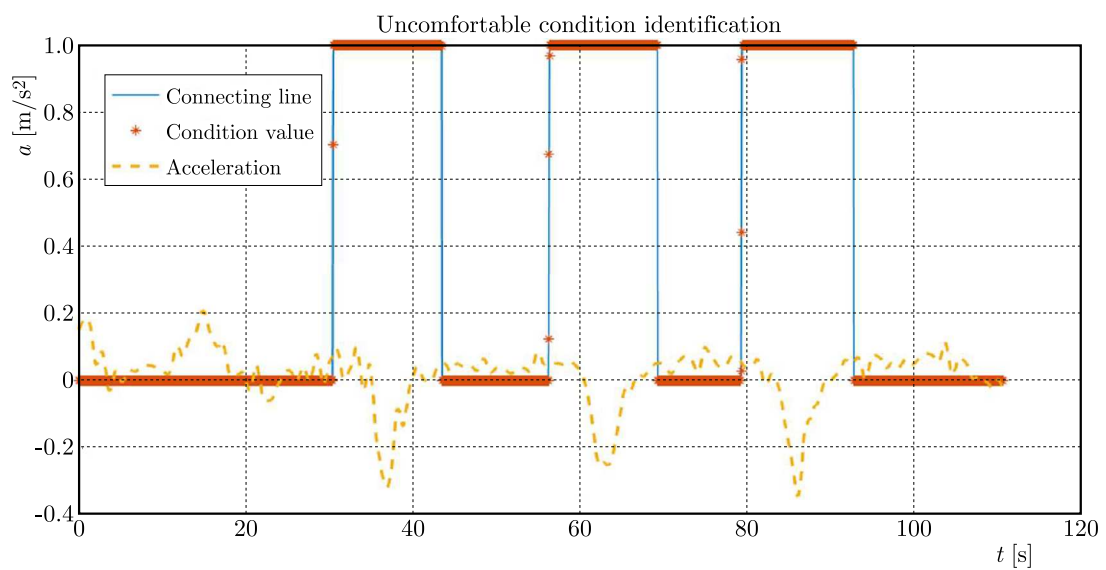


Fig. 13. Extraction of uncomfortable manoeuvres

perceived risks to drivers and passengers, and the braking process can be smoothed by braking in advance or increasing the following distance.

- The high accuracy identification network of uncomfortable manoeuvres is trained by an artificial intelligence algorithm. Through subjective verification, it can accurately identify uncomfortable working conditions. These preliminary results will provide new ideas and methods for the comfort research of intelligent driving vehicles, and the exploration of design evaluation of the human-machine system adaptability is carried out.

Acknowledgements

This study was supported by China Intelligent and Connected Vehicles (Beijing) Research Institute Co., Ltd. and the intelligent driving vehicle was provided by Great Wall Motors Co., Ltd.

References

1. ARCHER N.P., WANG S., 2010, Application of the back propagation neural network algorithm with monotonicity constraints for two-group classification problems, *Decision Sciences*, **24**, 1, 60-75
2. BURKHARD G., VOS S, MUNZINGER N., ENDERS E., SCHRAMM D., 2018, *Requirements on Driving Dynamics in Autonomous Driving with Regard to Motion and Comfort*, Springer Verlag
3. CAI S., LI K., SELESNICK I., 2003, *Matlab Implementation of Wavelet Transforms*, Electrical Engineering at Polytechnic University, NY
4. DIDIER M, LANDAU K., 2005, Influence of driver characteristics and driving environment on the comfort evaluation of ACC-System, [In:] *Adaptive Cruise Control*, Lea & Febiger
5. GUAN W., YAO Q., GAO Y., LU B., 2015, Transient power quality detection and location of distribution network based on db4 wavelet transform, *Dianli Xitong Baohu yu Kongzhi/Power System Protection and Control*, **43**, 8, 102-106
6. HAZARIKA N., CHEN J.Z., TSOI A.C., SERGEJEV A., 1997, *Classification of EEG signals using the wavelet transform*, *Signal Processing*, **59**, 1, 61-72
7. KUSMIREK S., HANA K., SOCHA V., PRUCHA J., KUTILEK P., SVOBODA Z., 2016, Postural instability assessment using trunk acceleration frequency analysis, *European Journal of Physiotherapy*, **18**, 4, 237-244
8. LIU L., JIE C., XU L., 2008, Realization and application research of BP neural network based on MATLAB, *International Seminar on Future Biomedical Information Engineering, IEEE*, 130-133
9. MOON T.K., STIRLING W.C., 2000, *Mathematical Methods and Algorithms for Signal Processing*, Prentice Hall
10. RIHACZEK A.W., 1968, Signal energy distribution in time and frequency, *IEEE Transactions on Information Theory*, **14**, 3, 369-374
11. RIOUL O., VETTERLI M., 1991, Wavelets and signal processing, *IEEE Signal Processing Magazine*, **8**, 4, 14-38
12. TANG T.-Q., ZHANG J., CHEN L., SHANG H.-Y., 2017, Analysis of vehicle's safety envelope under car-following model, *Physica A: Statistical Mechanics and its Applications*, **474**, 127-133
13. WANG Y., ZHANG Q., ZHANG L., HU Y., 2019, A method to automatic measuring riding comfort of autonomous vehicles: based on passenger subjective rating and vehicle parameters, [In:] *Design, User Experience, and Usability*, Springer International Publishing, 130-145
14. XING J.L., 2007, BP neural network pattern and application, *Journal of Shayang Teachers College*
15. YUSOF N.M., KARJANTO J., TERKEN J., DELBRESSINE F., HASSAN M.Z., RAUTERBERG M., 2016, The exploration of autonomous vehicle driving styles: preferred longitudinal, lateral, and vertical accelerations, *Proceedings of the 8th International Conference on Automotive User Interfaces and Interactive Vehicular Applications*, 245252

16. ZHANG W.J., YU S.X., PENG Y.F., CHENG Z.J., WANG C., 2015, Driving habits analysis on vehicle data using error back-propagation neural network algorithm, [In:] *Computing Control Information and Education Engineering*, H.-C. Liu, W.-P. Sung, W. Yao (Edit.), CRC Press
17. ZHAO S.M., 2006, Comparison of BP algorithms in Matlab NN toolbox, *Computer Simulation*
18. ZHAO Y., ZHANG Y.-H., LIN J.-H., 2013, Summary on the pseudo-excitation method for vehicle random vibration PSD analysis, *Applied Mathematics and Mechanics*, **34**, 2, 107-117

Manuscript received November 3, 2021; accepted for print April 4, 2022